THE ASTROPHYSICAL JOURNAL, 417:748–756, 1993 November 10

MAGNETIC RECONNECTION AT STRESSED X-TYPE NEUTRAL POINTS

L. OFMAN[1] AND P. J. MORRISON
Department of Physics and Institute for Fusion Studies, The University of Texas at Austin, Austin, TX 78712

AND

R. S. STEINOLFSON
Department of Space Sciences, Southwest Research Institute, San Antonio, TX 78228
Received 1992 October 21; accepted 1993 May 7

ABSTRACT

The reconnection and relaxation of two-dimensional stressed (nonpotential) X-type neutral point magnetic fields are studied via solution of the nonlinear resistive two-dimensional MHD equations and by analytical solution of the linear eigenvalue problem. Previous linear studies (Craig & McClymont 1991; Hassam 1992; Craig & Watson 1992), have shown that such stressed fields may relax on a time substantially shorter (i.e., $\sim|\log\eta|^2$, where η is the resistivity) than the usual time scale for linear reconnection (i.e., $\eta^{3/5}$). We have generalized the linear dispersion relation for azimuthally nonsymmetric perturbations and have found that for modes with azimuthal mode numbers $m > 0$, the relaxation can occur at a rate faster than that for $n = m = 0$, where n is the radial "quantum" number. All of the results presented are for frozen-in (line-tied) boundary conditions at some distance from the X-point, and we emphasize that these boundary conditions are essential in order to obtain our solutions. We find that for nearly azimuthally symmetric magnetic perturbations the fields relax incompressibly and nonlinearly to the unstressed X-type neutral point at a rate close to that predicted by linear theory. Also, fully compressible nonlinear MHD simulations have been performed, which show that the interaction between the plasma flow velocity and the magnetic field is the important physical effect, while the inclusion of thermodynamics does not affect the evolution considerably. A Liapunov functional for the nonlinear incompressible two-dimensional resistive MHD equations is derived to show that the current-free X-point configuration is a global equilibrium to which general initial conditions relax.

Subject heading: MHD

1. INTRODUCTION

Magnetic reconnection is believed to occur in several natural phenomena, including solar coronal loops, the magnetopause boundary, the solar wind, extragalactic jets, and fusion experiments. Giovanelli (1947) was the first to observe that solar flares frequently occur near magnetic neutral points. Based on these observations Dungey (1953, 1958) proposed an X-type neutral point mechanism for particle acceleration, the onset of sheet currents, and the energy release in solar flares, provided that the magnetic field sources are free to move. Chapman & Kendall (1962) solved the nonlinear ideal MHD equations for an unbound plasma with the X-type neutral point and found growth on an Alfvén time scale, while Syrovatsky (1966, 1971) included the mechanism in a solar flare model. Sweet (1958) and Parker (1963) used dimensional arguments for a model involving merging of antiparallel magnetic fields and concluded that the reconnection rate scales as $\eta^{1/2}$, while Petschek (1964) predicted an Alfvénic reconnection rate based on semiquantitative Alfvén shock wave solutions. Furth, Killeen, & Rosenbluth (1963) developed an analytic boundary layer theory and derived the $\eta^{3/5}$ linear tearing growth rate scaling, while Rutherford (1973) considered the nonlinear stage and found that the reconnected flux $\Phi \sim \eta t$ and the reconnection rate diminishes from an exponential to an algebraic rate. Biskamp (1986) studied the magnetic reconnection via current sheets, using the two-dimensional incompressible MHD approach with plasma and magnetic flux injected at the boundaries. His results agree with the Sweet (1958) and Parker (1963) slow reconnection rate. DeLuca & Craig (1992) used the two-dimensional incompressible MHD approach with periodic boundary conditions and found that the ohmic dissipation rate is fast (i.e., approximately independent of resistivity) and reconnection rate scales as $\eta^{1/4}$. We would like to emphasize that the different reconnection rate scalings mentioned above were obtained with different boundary and initial conditions.

The existence of fast magnetic reconnection in space and astrophysical plasma is still an open question. Recently, Hassam (1992) has considered an X-point magnetic field configuration with frozen-in boundary conditions and has analytically solved the linearized, compressible, low-β MHD equations (where β is the ratio of the gas to the magnetic pressure of the plasma) for azimuthally symmetric ($m = 0$) modes. An independent study by Craig & McClymont (1991, 1993) and Craig & Watson (1992) finds that the perturbed X-point with an intermediate decay rate that is slower than the Alfvén rate but faster than the resistive diffusion rate. Craig & McClymont (1991, 1993) and Craig & Watson (1992) find that the asymptotic reconnection rate for the linearized X-point problem is always fast and scales as $|\log\eta|^2$ in exact agreement with Hassam (1992), while the nonreconnective modes relax asymptotically on the $|\log\eta|^3$ time scale. The results of the present study agree with the above relaxation rates. Experimental studies by Bratenahl & Yeates (1970), Baum & Bratenahl (1974a, b), and Baum, Bratenahl, & White (1973) and Baum & Pollack (1973) found that the initially perturbed X-type magnetic field configuration rapidly relaxes to the potential state. For a detailed review, see, for example, Priest (1981), Syrovatsky (1981), and references therein.

[1] Present address: NASA/Goddard Space Flight Center, Code 682.1, Greenbelt, MD 20771.

This is a first study of X-point reconnection with the two-dimensional, nonlinear, resistive MHD equations for both incompressible and fully compressible (without restrictions on the value of the pressure) plasma with the frozen-in boundary condition. Both the linear and nonlinear relaxation rates of the stressed (perturbed) X-point back to the potential X-point configuration are obtained. In addition, we have obtained a general dispersion relation that includes the azimuthally nonsymmetric ($m > 0$) modes, as well as the $m = 0$ mode, and have compared the results of the linear dispersion relation with the nonlinear simulations. By considering compressible (low-β and $\beta = 0.1$) and incompressible dynamics, we show that the essential physics is dominated by the coupling of the magnetic field to the inertial terms, and that gas pressure gradients do not preclude the relaxation process. Finally, we obtain a Liapunov functional for the nonlinear, incompressible two-dimensional resistive MHD equations, which shows that the potential X-point with the frozen-in boundary conditions is an equilibrium state to which all initial conditions relax.

The effect of free boundary conditions; i.e., where the plasma is allowed to flow through the boundary and where the magnetic field at the boundary is free to adjust, was considered in separate studies (Ofman 1992; Steinolfson, Ofman, & Morrison 1992). There it was found that the X-point evolves into a current sheet and the perturbation grows (rather than relaxes) on an Alfvén time scale.

This paper is organized as follows: In § 2 the basic MHD equations for our model and the initial magnetic field configuration are presented. In § 3 we derive the linear dispersion relation. The numerical results of the nonlinear MHD simulations are presented in § 4, and the summary and discussion are in § 5. The Liapunov relaxation arguments are given in the Appendix.

2. INCOMPRESSIBLE TWO-DIMENSIONAL MHD EQUATIONS

We assume that collisional MHD theory (Drake & Lee 1977) is applicable, that the plasma resistivity η is constant and isotropic, and that gravitational and viscous effects are negligible. With these assumptions the basic equations in cgs units are

$$\rho\left[\frac{\partial \boldsymbol{v}}{\partial t} + (\boldsymbol{v}\cdot\nabla)\boldsymbol{v}\right] = -\nabla P + \frac{1}{4\pi}(\nabla\times\boldsymbol{B})\times\boldsymbol{B}\,, \tag{2.1}$$

$$\frac{\partial \boldsymbol{B}}{\partial t} = \nabla\times(\boldsymbol{v}\times\boldsymbol{B}) - \frac{c^2\eta}{4\pi}\nabla\times(\nabla\times\boldsymbol{B})\,, \tag{2.2}$$

$$\frac{\partial \rho}{\partial t} + \nabla\cdot(\rho\boldsymbol{v}) = 0\,, \tag{2.3}$$

$$\nabla\cdot\boldsymbol{B} = 0\,, \tag{2.4}$$

$$\frac{d}{dt}\left(\frac{p}{\rho^{\gamma_p}}\right) = 0\,, \tag{2.5}$$

where c is the speed of light, ρ is the plasma density, $\boldsymbol{B}$ is the magnetic field, $\boldsymbol{v}$ is the velocity field, P is the pressure, and γ_p is the polytropic index. We use equations (2.1)–(2.5) with the equilibrium of equation (2.8) below. Assuming that the evolution is two-dimensional ($\partial/\partial z = 0$), the above set of equations is solved using three separate approaches:

1. Solution of the dispersion relation arising from the linearized equations (2.1)–(2.4), with the assumption $\nabla P = 0$ in equation (2.1); the low-β approximation.

2. Numerical solution of the two-dimensional MHD equations in slab geometry given below in equations (2.9) and (2.10), which are obtained from equations (2.1)–(2.4) with the assumption of incompressibility ($\nabla\cdot\boldsymbol{v} = 0$).

3. Numerical solution of the compressible MHD equations (2.1)–(2.3) and equation (2.5) in the (r, θ) plane without any further approximations (eq. [2.4] is not solved explicitly).

The linearized equations resulting from the first approach and their solution will be presented in § 3. In the remainder of this section we present the equations needed for the second approach.

In two dimensions the magnetic and velocity fields can be written as

$$\boldsymbol{B} = \nabla\Psi\times\boldsymbol{e}_z \tag{2.6}$$

$$\boldsymbol{V} = \nabla\phi\times\boldsymbol{e}_z \tag{2.7}$$

where Ψ and ϕ are the flux and stream functions, respectively, and $\Psi = \psi_E + \psi$ with the equilibrium stream function ψ_E given by

$$\psi_E = B_0(x^2 - y^2)/2a\,. \tag{2.8}$$

Next, substituting equations (2.6)–(2.8) into equations (2.1) and (2.2) with $\rho = \rho_0 = \text{const}$, and taking the curl of equation (2.1) to eliminate the pressure P, yields the following set of equations, which we write in dimensionless form:

$$\frac{\partial\psi}{\partial t} = -\frac{\partial\phi}{\partial y}\left(\frac{\partial\psi}{\partial x} + x\right) + \left(\frac{\partial\psi}{\partial y} - y\right)\frac{\partial\phi}{\partial x} - \frac{1}{S}J \tag{2.9}$$

$$\frac{\partial\omega}{\partial t} = -\frac{\partial\phi}{\partial y}\frac{\partial\omega}{\partial x} + \frac{\partial\phi}{\partial x}\frac{\partial\omega}{\partial y} + \left(\frac{\partial\psi}{\partial y} - y\right)\frac{\partial J}{\partial x} - \left(\frac{\partial\psi}{\partial x} + x\right)\frac{\partial J}{\partial y}\,, \tag{2.10}$$

where $J = -\nabla_\perp^2\psi$ is the z-component of the current, $\omega = -\nabla_\perp^2\phi$ is the z-component of the vorticity, and $\nabla_\perp^2 \equiv (\partial^2/\partial x^2) + (\partial^2/\partial y^2)$ with $\partial/\partial z = 0$. The time is normalized to the Alfvén time $\tau_h = a_b(4\pi\rho_0)^{1/2}/B_0$, the coordinates are scaled by the characteristic magnetic field length a_b, and B_0 is the average magnitude of the magnetic field at the boundary. The dimensionless parameter in these equations is the magnetic Reynolds number $S = \tau_r/\tau_h$, where $\tau_r = 4\pi a_b^2/c^2\eta$ is the resistive diffusion time. We have also assumed that the equilibrium magnetic field is maintained by an external electric field (i.e., the equilibrium magnetic field is not dissipated resistively). In § 4 we present the numerical results obtained with equations (2.9) and (2.10).

3. LINEAR DISPERSION RELATION

In the present section we extend the compressible low-β azimuthally symmetric ($m = 0$) linear dispersion relation for the X-point (Hassam 1992) to non-azimuthally symmetric arbitrary m modes. The linearized, low-β, MHD equations combine into a single differential equation for ψ given by (Hassam 1992; Craig & McClymont 1991)

$$\frac{\partial^2\psi}{\partial t^2} - S^{-1}\frac{\partial}{\partial t}\nabla^2\psi = |\nabla\psi_E|^2\nabla^2\psi\,, \tag{3.1}$$

where $|\nabla\psi_E|^2 = r^2 = x^2 + y^2$. The diffusion term in equation (3.1) is dominant when $r \ll r_c$, where $r_c = \eta^{1/2} = S^{-1/2}$ is the skin depth (η is the dimensionless resistivity). Assuming the following separation of variables in cylindrical geometry

$\psi(r, \theta, t) = e^{-\gamma t} f(r) e^{im\theta}$, the eigenvalue equation for $f(r)$ becomes (Craig & McClymont 1991)

$$r \frac{d}{dr}\left(r \frac{df}{dr}\right) = \left(\frac{\gamma^2}{1 - \gamma/Sr^2} + m^2\right) f , \tag{3.2}$$

and the radial variation of the current $\boldsymbol{j} = -\nabla^2 \psi \boldsymbol{e}_z$ is given by

$$j(r) = \frac{\gamma^2}{\gamma/S - r^2} f(r) . \tag{3.3}$$

The frozen-in boundary condition is given by

$$f(r = 1) = \psi(r = 1, \theta) = 0 . \tag{3.4}$$

Equation (3.2) is mapped into the hypergeometric equation by the transformations $z = r^2 S/\gamma$, and $f = z^{\alpha}\xi$:

$$z(z - 1)\xi'' + (m + 1)(z - 1)\xi' - \gamma^2/4\xi = 0 , \tag{3.5}$$

where we have set $\alpha = m/2$. The solution of equation (3.5) that is regular at $r = 0$ is the hypergeometric function $F(a, b, c, z)$ with $a = m/2 + \Delta/2$, $b = m/2 - \Delta/2$, $c = m + 1$, and $\Delta = (m^2 + \gamma^2)^{1/2}$. From the boundary condition (3.4) we obtain the dispersion relation

$$F(m/2 + \Delta/2, m/2 - \Delta/2, m + 1, S/\gamma) = 0 . \tag{3.6}$$

For the cases of interest at $r = 1$, $|z| = |S/\gamma| > 1$; hence, the transformation formula (Oberhettinger 1972)

$$F(a, b, c, z) = \frac{\Gamma(c)\Gamma(b - a)}{\Gamma(b)\Gamma(c - a)} (-z)^{-a} \times F\left(a, 1 - c + a, 1 - b + a, \frac{1}{z}\right) + \frac{\Gamma(c)\Gamma(a - b)}{\Gamma(a)\Gamma(c - b)} \times (-z)^{-b} F\left(b, 1 - c + b, 1 - a + b, \frac{1}{z}\right), \quad |\arg(-z)| < \pi \tag{3.7}$$

is needed to obtain the dispersion relation. Substituting the values of a, b, and c, using the properties of the gamma function, and using equation (3.6) yields the following linear dispersion relation for the X-point:

$$\frac{(m + \Delta)\Gamma(-\Delta)\Gamma^2(m/2 + \Delta/2)}{(m - \Delta)\Gamma(\Delta)\Gamma^2(m/2 - \Delta/2)} = -\left(-\frac{S}{\gamma}\right)^{\Delta} \frac{F(m/2 - \Delta/2, -m/2 - \Delta/2, 1 - \Delta, \gamma/S)}{F(m/2 + \Delta/2, -m/2 + \Delta/2, 1 + \Delta, \gamma/S)} . \tag{3.8}$$

Equation (3.8) can be further simplified with the assumption $\gamma/S \ll 1$, which results in the following upon asymptotically expanding the right-hand side of equation (3.8)

$$\frac{(m + \Delta)\Gamma(-\Delta)\Gamma^2(m/2 + \Delta/2)}{(m - \Delta)\Gamma(\Delta)\Gamma^2(m/2 - \Delta/2)} \approx -\left(-\frac{S}{\gamma}\right)^{\Delta} \frac{1 + [\gamma^3/4S(1 - \Delta)]}{1 + [\gamma^3/4S(1 + \Delta)]} . \tag{3.9}$$

When $m = n = 0$ and in the limit $|\gamma| \ll 1$, the dispersion relation (3.8) can be approximated by the following asymptotic expressions (Hassam 1992):

$$\mathrm{Im}\ \gamma \sim \frac{\pi}{\log S}\left[1 - \frac{\log(\log S)}{\log S}\right] \tag{3.10}$$

$$\mathrm{Re}\ \gamma \sim \frac{\psi/2}{\log S}\ \mathrm{Im}\ \gamma \sim \frac{\pi^2}{2(\log S)^2} . \tag{3.11}$$

For an arbitrary m and in the limit of low resistivity, Craig & McClymont (1993) obtained the following expression by matching the solutions in the diffusion region ($r < r_c$) to the outer region solutions ($r > r_c$):

$$\mathrm{Re}\ \gamma \sim \frac{k^3}{4\omega n^*} , \tag{3.12}$$

where $n^* = n + 1 - \frac{1}{2}\delta_{0,m}$, $n = 0, 1, 2, \ldots$, $\omega^2 = k^2 + m^2$, and $k \approx 2n^*\pi/|\log S|$. Their asymptotic expression can be derived from our dispersion relation in the limit of large S by taking the log on both sides of equation (3.8), noting the phase change of the left-hand side for $m > 0$, equating the real and imaginary parts, and solving iteratively for Re γ. The values of γ calculated from equation (3.12) agree with our dispersion relation (3.8) in the limit of small resistivity.

We have solved the exact dispersion relation (3.8) numerically for $m = 0$ and several $m > 0$ modes, with S varying over 10 orders of magnitude. Values of γ from equations (3.10) and (3.11) were used as initial guesses in our numerical solution of the exact dispersion relation. The resulting decay rates and their dependence on S, with $m = n = 0$ and $n = 1$, $m = 2, 4$ are shown in Figure 1. The near linear dependence of Re γ for the various modes is in general agreement with the log S scaling of the decay rate in equations (3.10)–(3.12). The best-fit powers of log S are 1.94 for the $m = 0$ mode, 3.01 for the $m = 2$ mode, and 3.65 for the $m = 4$ mode.

The real and imaginary parts of the eigenfunction $f(r)$, and the radial variation of the current $j(r)$ with $m = 0$, $n = 1$, $S = 10^3$ and $m = 1$, $n = 3$, $S = 10^5$ are presented in Figure 2. The "quantum" number n determines the number of radial nodes of $f(r)$ in the interval $r\epsilon(0, 1)$ and corresponds to distinct branches of the complex dispersion relation (3.8). When $m = 0$,

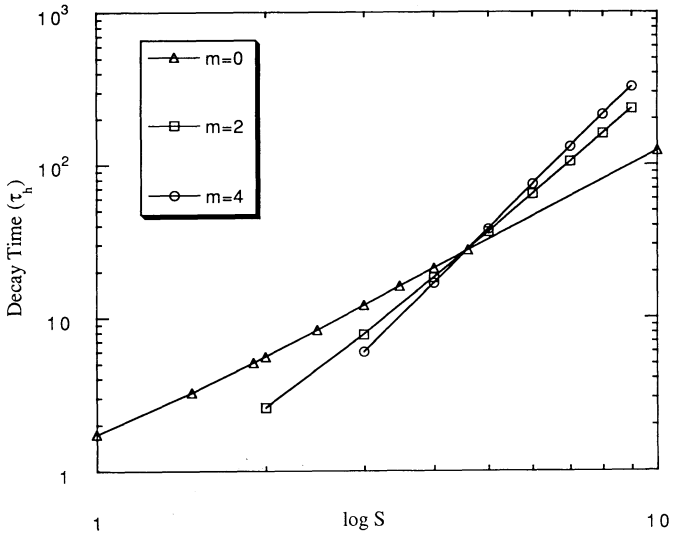

FIG. 1.—Decay rates of the modes with $m = n = 0$, and $n = 1$, $m = 2, 4$ obtained from the solution of the linear dispersion relation (3.8).

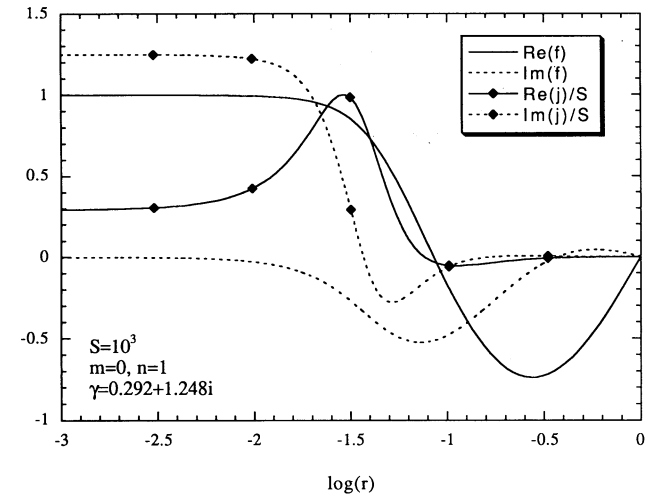

FIG. 2a

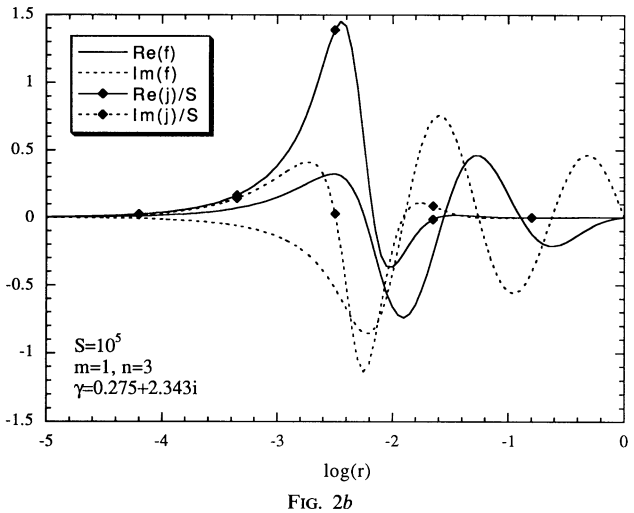

FIG. 2b

FIG. 2.—The real and imaginary parts of the eigenfunctions $f(r)$ and the current $j(r)$. (*a*) $m = 0$, $n = 1$, $S = 10^3$, $\gamma = 0.292 + 1.248i$. (*b*) $m = 1$, $n = 3$, $S = 10^5$, $\gamma = 0.275 + 2.343i$.

Re $\{f(r)\}$ approaches a constant as $r \to 0$ and when $m = 1$, $f(r \to 0) \to 0$. It is evident from equation (3.3) that the current j becomes proportional to $f(r)$ as r approaches zero; therefore, for the $m = 0$ mode $j(r \to 0) \to$ const, and for the $m = 1$ mode $j(r \to 0) \to 0$. The $m > 0$ modes are not associated with reconnection at the X-point in agreement with previous studies (Hassam 1992; Craig & McClymont 1991; Craig & Watson 1992); however, these modes decouple the fluid motion from the magnetic field, thus generating very large currents in the vicinity of the X-point [near the extrema of $f(r)$]. The plasma motions are heavily damped by the restoring $\boldsymbol{j} \times \boldsymbol{B}$ force and relax on the fast $\sim(\log S)^3$ time scale.

In Figure 3 the solution of the exact dispersion relation for the $n = m = 0$ modes is compared with the asymptotic expression (3.11) for $10 \leq S \leq 10^{100}$ and with the decay rates obtained from the incompressible MHD simulation. For $S = 10^4$ (characteristic of laboratory plasmas) the $n = m = 0$ perturbation decay time is about 20 Alfvén times with a similar oscillation period. For $S = 10^{10}$ (a typical value for the solar coronal plasma) the $n = m = 0$ perturbation decay time is about 120 Alfvén times and is longer than two oscillation periods. Very good agreement is seen between the nonlinear simulation with $10^2 \leq S \leq 4 \times 10^4$, the exact dispersion relation, and the asymptotic expression. The nonlinear terms in the MHD simulations become smaller as the perturbation decays, and the decay rates approach the linear rate. The asymptotic nature of equation (3.11) is evident in Figure 3 since agreement with the dispersion relation is improved at very large values of S.

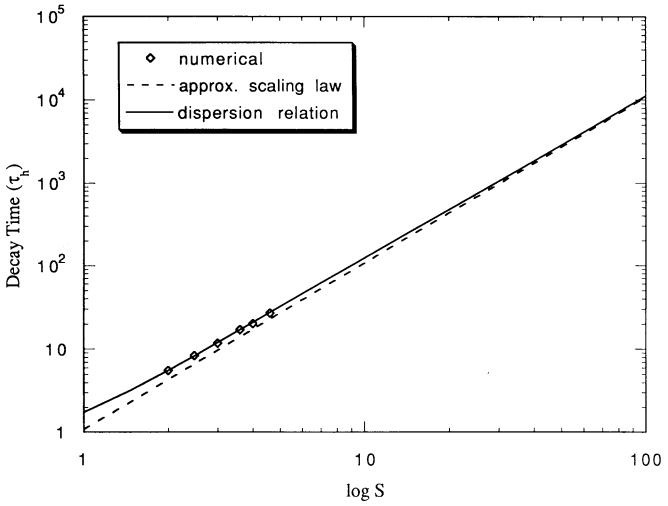

FIG. 3.—Scaling of the decay rate with S for the $m = n = 0$ mode. The solid curve represents the solution of the linear dispersion relation (3.8), the dashed curve is the asymptotic log S scaling (3.11), and the squares represent the decay times obtained from the incompressible simulations.

4. NONLINEAR SIMULATIONS

4.1. *Incompressible MHD*

Now we describe results obtained by using the alternative direction implicit (ADI) method to solve the incompressible two-dimensional MHD equations (2.9) and (2.10) in slab geometry. The method of solution was discussed in detail in Ofman (1992), and the code was applied successfully to study nonlinear tearing modes (Steinolfson & Van Hoven 1984; Ofman, Morrison, & Steinolfson 1993). As an additional test of the code we have obtained solutions with periodic boundary conditions and recovered the results of DeLuca & Craig (1992) for magnetic reconnection in incompressible fluids. Here we have imposed the frozen-in and ideal fluid boundary conditions in x- and y-directions, respectively; namely,

$$\psi(x = \pm x_{\max}, y) = \phi(x = \pm x_{\max}, y) = \psi(x, y = \pm y_{\max}) = \phi(x, y = \pm y_{\max}) = 0 . \quad (4.1)$$

The calculations are initiated with a small perturbation ψ that satisfies the boundary conditions (4.1), and that is nearly azimuthally symmetric in the vicinity of the X-point. In particular we choose

$$\psi(x, y, t = 0) = be^{-5(x^2+y^2)}(x_{\max}^2 - x^2)(y_{\max}^2 - y^2) , \quad (4.2)$$

with $b \ll 1$ and $x_{\max} = y_{\max} = 0.5$. In contrast to the previous incompressible studies (e.g., Biskamp 1986; DeLuca & Craig 1992), our frozen-in and ideal fluid boundary conditions (4.1) do not allow flux or mass flow through the boundaries.

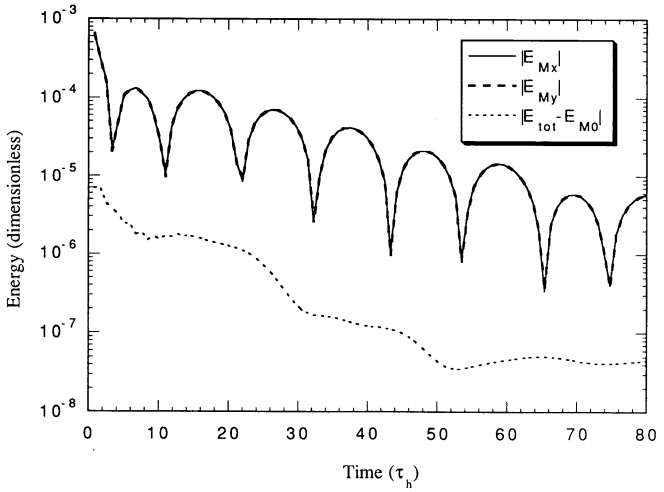

FIG. 4.—The absolute values of the excess magnetic energies E_{Mx} (*solid line*), E_{My} (*long dashed line*), and the excess total energy $E_{tot} - E_{M0}$ (*short dashed line*).

Figures 4–5 show the incompressible relaxation of an X-point with the above boundary and initial conditions for $S = 10^4$. In Figure 4 plots of the perturbed energies stored in the x- and y-components of the magnetic field and the total energy are displayed as functions of time. The perturbed energy stored in the magnetic field is given by

$$E_M(t) = E_{Mx} + E_{My} = \int_{-x_{max}}^{x_{max}} \int_{-y_{max}}^{y_{max}} \left[\left(\frac{\partial \psi}{\partial y} - y \right)^2 + \left(\frac{\partial \psi}{\partial x} + x \right)^2 - y^2 - x^2 \right] dx\, dy \,, \quad (4.3)$$

The perturbed kinetic energy is given by

$$E_K(t) = \int_{-y_{max}}^{y_{max}} \int_{-x_{max}}^{x_{max}} \left[\left(\frac{\partial \phi}{\partial y} \right)^2 + \left(\frac{\partial \phi}{\partial x} \right)^2 \right] dx\, dy \,, \quad (4.4)$$

and the total energy is given by

$$E_{tot}(t) = E_M(t) + E_K(t) + E_{M0} \,, \quad (4.5)$$

where E_{M0}, the energy stored in the initial magnetic field configuration, is given by

$$E_{M0} = \int_{-x_{max}}^{x_{max}} \int_{-y_{max}}^{y_{max}} [y^2 + x^2] dx\, dy = \tfrac{4}{3} x_{max}\, y_{max} (x_{max}^2 + y_{max}^2) \,. \quad (4.6)$$

Because of resistive dissipation E_{tot} satisfies

$$\frac{dE_{tot}}{dt} = -2 \int_{-y_{max}}^{y_{max}} \int_{-x_{max}}^{x_{max}} S^{-1} J^2\, dx\, dy \,; \quad (4.7)$$

we have neglected viscous dissipation since the simulation algorithm is nearly ideal (Ofman et al. 1991). The energies in equations (4.3)–(4.7) are scaled by $B_0^2/8\pi$. The perturbed energies are transferred alternately between the x-component (*solid curve*) and y-component (*long dashes*) of the magnetic field. The total energy (*short dashes*) is conserved within the anticipated resistive dissipation rate of 2 Re $\gamma \approx 0.1$ (see eq. [4.7]) and most of the energy is dissipated within the first two oscillation periods ($t \approx 50\tau_h$). It is interesting to note the steplike nature of the energy dissipation. Similar steplike time dependence of the total energy was found by Craig & Watson (1992) in their compressible MHD reconnection studies. This feature is due to the uncoupling of the fluid motion from the magnetic field in the presence of small resistivity.

Figure 5 shows the absolute values of $\psi(0, 0, t)$ (*solid curve*), and the reconnected flux (*dashed curve*) defined by

$$\Delta\Phi(t) \equiv \int_{-x_{max}}^{x_{max}} \left| \frac{\partial}{\partial x'} \psi(x', 0, t) \right| dx' + \int_{-y_{max}}^{y_{max}} \left| \frac{\partial}{\partial y'} \psi(0, y', t) \right| dy' \,. \quad (4.8)$$

The decay rate and the oscillation frequency are determined from $\psi(0, 0, t)$ using the method described in Ofman et al. (1991). The relaxation rate of the X-point ($\gamma = 0.053 + 0.297i$) obtained from $\psi(0, 0, t)$ agrees well with the decay rate ($\gamma = 0.048 + 0.292i$) obtained from the solution of the dispersion relation with $m = n = 0$. The good agreement with the linear dispersion relation was found to hold for more than 2.5 orders of magnitude of S that were considered in this study (see Fig. 3).

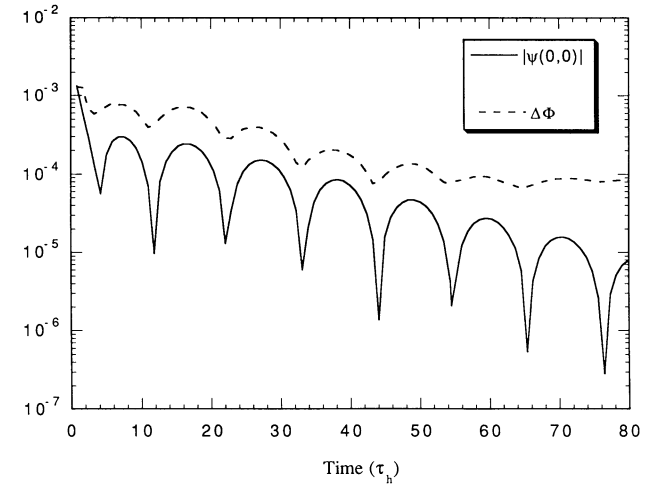

FIG. 5.—The absolute values of $\psi(0, 0, t)$ (*solid line*) and the reconnected flux (*dashed line*).

4.2. *Compressible MHD*

Equations (2.1)–(2.3) and equation (2.5) were solved using the Lax-Wendroff differencing scheme in a manner similar to that given by Richtmyer & Morton (1967), along with a smoothing term suggested by Lapidus (1967). The computation is done in polar coordinates (r, θ) in the domain $0 \le \theta \le \pi$, $0 \le r \le 1$. The code was previously tested and successfully applied to other MHD problems (Steinolfson & Winglee 1993). Here the code is used with the frozen-in boundary conditions at the outer boundary $r = 1$, $0 \le \theta \le \pi$, and symmetry boundary conditions at the diameter $0 \le r \le 1$, $\theta = 0, \pi$. The equilibrium magnetic field in cylindrical geometry is given by

$$\boldsymbol{B}_E = r(\sin 2\theta \boldsymbol{e}_r + \cos 2\theta \boldsymbol{e}_\theta) \,, \quad (4.9)$$

and the corresponding flux function is $\psi_E = -\frac{1}{2} r^2 \cos(2\theta)$. We have initiated the computations with the following perturbations: for the $m = 0$ case

$$\psi = -\frac{b}{\pi} [1 + \cos(\pi r)] \quad (4.10)$$

is used, while the $m > 0$ computations are initiated with

$$\psi = br^3(1 - r)^3 \cos(m\theta) \,, \quad (4.11)$$

where b is a parameter that controls the magnitude of the initial perturbation (and hence the "nonlinearity" of the initial

state). The particular choices of ψ are zero at $r = 1$, and they yield a zero current at the boundary. For $m > 0$ modes ψ and j also vanish at the origin. The simulations are evolved until the magnetic field configuration reaches a steady state (i.e., relaxes to the current-free X-point).

The temporal evolution of the magnetic field at $r_i = 0.02$, 0.04, 0.06, 0.08, 0.1, and $\theta = \pi/2$ is shown in Figures 6*a*–6*c* (curves A-E, respectively), with $S = 10^4$. The reference $\beta = 0.1$ and the Alfvén time $\tau_h = 11$ s based on the magnetic field at the boundary. The values shown are $\Delta B_\theta \equiv |[B_\theta(r_i, \theta, t) - B_\theta(r_i, \theta, 2)]/B_\theta(r_i, \theta, 2)|$, where $B_\theta = -(\partial\Psi/\partial r)$ with an $m = 0$ initial perturbation in Figures 6*a*–6*b* and $m = 2$ initial perturbation in Figure 6*c*. The fields oscillate almost in phase at r_i, and the frequency agrees well with that predicted by linear theory (with the period of $T = 0.60$ minutes and $T = 0.42$ minutes for $m = 0$ and $m = 2$ modes, respectively). The minor phase difference and the higher harmonics are due to nonlinear effects and can be made arbitrary small by reducing the magnitude of the initiating perturbation. In Figure 6*b* the initial $m = 0$ perturbation is two orders of magnitude smaller than that of Figure 6*a*, and the evolution of ΔB_θ at r_i approaches that expected from linear theory. The nonoscillatory decay phase of the $m = 0$ mode at large t appears after most of the flux was reconnected in the oscillatory phase (see also $|\Delta\Phi|$ at $t > 60\tau_h$ in Fig. 5). The long decay tail of ΔB_θ can be identified with similarity solutions of the linearized low-β MHD equations (see Hassam 1992 for detailed discussion).

The decay rates obtained from the $\beta = 0.1$ computations are faster then rates obtained from the low-β linear theory. This result seems to be in disagreement with previous studies by Craig & Watson (1992) who claim that finite gas pressure can preclude the fast reconnection rate. At present we do not fully understand the differences between our results and those of Craig & Watson. It should be noted, however, with the two-dimensional X-point equilibrium $B_E^2 \sim r^2$ and the radial dependence of β is $\beta(r) \sim \beta/r^2$. Therefore, the plasma is dominated by thermal pressure for $r \leq r_c$ even for extremely low values of $\beta > S^{-1}$ at the boundary. For the present example $\beta(r = r_c) = 10^3$! In addition, ∇P does not even appear in the basic low-β theory (Craig & McClymont 1991; Hassam 1992), and to the extent that this assumption approximates the essential physics, one would expect that the thermal pressure would not be important. It is evident that additional finite-β studies are needed in particular with more realistic magnetic field configuration (e.g., including finite B_z component).

5. SUMMARY AND DISCUSSION

We have derived the linear dispersion relation for the relaxation rate of an X-type neutral point with frozen-in boundary conditions for modes with any value of m. The asymptotic reconnection rate for $m = 0$ modes scales as $(\log S)^{-2}$ in agreement with previous studies (Hassam 1992; Craig & McClymont 1991). When the $m > 0$ modes are present, large currents are generated at $r \approx r_c$, where $r_c = S^{-1/2}$ and the perturbations relax through the coupling of the fluid motions to the magnetic field via the $\boldsymbol{j} \times \boldsymbol{B}$ force at an asymptotic rate that scales as $(\log S)^{-3}$ in agreement with Craig & McClymont (1993). Although the $m > 0$ modes do not reconnect at $r = 0$, they can generate additional X-points away from the origin at the separatrices.

Numerical solution of the dispersion relation agrees with the asymptotic expressions for the decay rate. We have solved the nonlinear incompressible resistive two-dimensional MHD equations (2.9) and (2.10) in slab geometry using the ADI method. The computations were initiated with small, nearly azimuthally symmetric perturbations of ψ, with $\phi = 0$, for several values of the magnetic Reynolds number in the range $10^2 \leq S \leq 4 \times 10^4$. We have found that the perturbations decay in agreement with the linear dispersion relation for $n = m = 0$ modes. Namely, for large S the decay rate obtained from the incompressible MHD simulations scales as $(\log S)^{-2}$.

We have solved the compressible resistive two-dimensional MHD equations in the (r, θ) plane using the Lax-Wendroff differencing scheme with $S = 10^4$, $\beta = 0.1$, and $m = 0$, 1, 2 initial perturbations. We have found that with frozen-in boundary conditions the perturbed X-point relaxes to the potential X-point in agreement with the linearly predicted evolution. By obtaining the Liapunov functional of the current-free X-point with frozen-in boundaries we showed that this is an equilibrium configuration to which all perturbed states must relax (see Appendix).

The reconnection rate obtained from the linear theory and the nonlinear simulations is faster than the Sweet (1958) and Parker (1963) $\eta^{1/2}$ rate, but slower than the Petschek (1964) Alfvénic driven reconnection rate. The $m > 0$ modes relax faster than the $m = 0$ modes for $S < 10^4$. For typical solar parameters ($S = 10^{14}$), the $m = 0$ modes reconnect and dissipate most of their energy within a 100 Alfvén times, while the $m = 1$, 2 modes have a relaxation time which is an order of magnitude longer.

It is important to point out that the boundary conditions can play a crucial role in determining the reconnection rate. In the present study we imposed the frozen-in boundary conditions and obtained the fast reconnection rate in both compressible and incompressible solutions, and the predictions of the linear model appears to hold even for plasmas of finite gas pressure. We have shown how a perturbed X-point equilibrium subject to the frozen-in boundary conditions relaxes back to an equilibrium. Our linear analytic solutions would not be obtained without the form of boundary conditions used, which is also the case for the earlier studies by Hassam (1992), Craig & McClymont (1991, 1993), and Craig & Watson (1991). We followed the analytic study with numerical simulations of the MHD equations with more physics included than was in the linear study. Our simulations verified the linear results and also showed that the fast relaxation rate was not substantially affected by thermodynamic effects, such as pressure gradients. However, there are a couple of very important points to bear in mind in attempting to compare these results with other simulation studies (e.g., Biskamp 1986) or to apply them to various physical phenomena, such as the solar flare. First of all, there is absolutely no reason to expect that these results for the form of boundary conditions used would have any relation to other studies either for open boundaries or for driven reconnection where an inflow is imposed on the boundary. In fact, the work by Ofman (1992) and Steinolfson et al. (1992) shows dramatically different results for this problem when the boundary conditions are open. Similarly, these results would not necessarily apply to steady state reconnection. Finally, a relaxation phenomenon such as that considered here would not have immediate application to an explosive phenomenon such as a solar flare.

One of us (L. O.) would like to thank F. Porcelli for useful discussions. Another of us (P. J. M.) would like to acknowledge a conversation with A. Hassam that instigated the calculation in the Appendix. This work was supported by the US Department of Energy contract DE-FG05-80ET-53088 and the National Science Foundation contract ATM-90-15705.

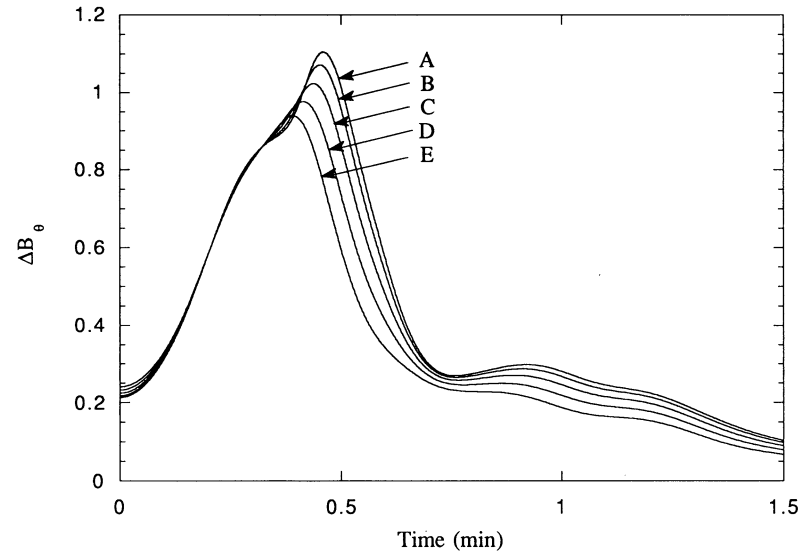

FIG. 6*a*

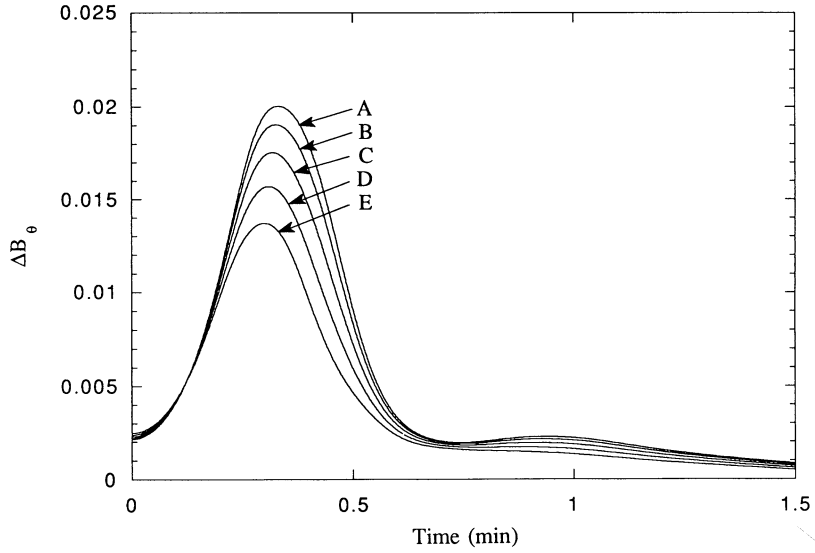

FIG. 6*b*

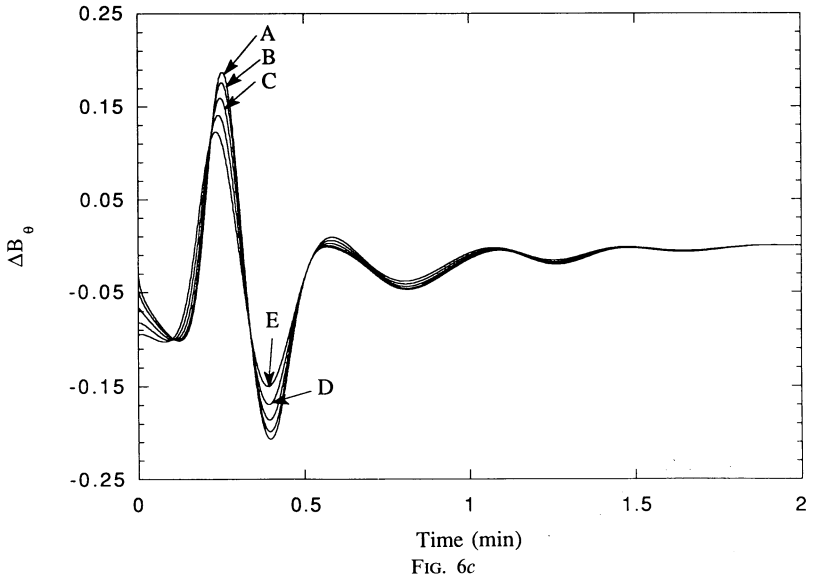

FIG. 6*c*

FIG. 6.—Compressible MHD simulation results for the relaxation of the X-point with $m = 0$ initial perturbation. (*a*) The change of the magnetic field ΔB_θ at $r_i = 0.02, 0.04, 0.06, 0.08, 0.1, \theta = \pi/2$. (*b*) Same as (*a*) with an initial perturbation which is two orders of magnitude smaller. (*c*) ΔB_θ with $m = 2$ initial perturbation.

APPENDIX

LIAPUNOV RELAXATION FOR INCOMPRESSIBLE MHD

In this appendix we present a formal Liapunov functional stability argument, which indicates that perturbations about the X-point equilibrium of equation (2.8) relaxes back to the original equilibrium state. The arguments used are akin to those employed for the well-known Boltzmann H-theorem of kinetic theory, which demonstrates relaxation to thermal equilibrium. Namely, if one can find a function, say H, defined on the state space of such a system, where contours of H are nested closed surfaces about the equilibrium point, which is a minimum, and where the time derivative $dH/dt \leq 0$ and vanishes only on the equilibrium point, then Liapunov's theorem guarantees asymptotic stability; i.e., the system approaches the equilibrium point as time approaches infinity.

The dynamics considered here is determined by the partial differential equations of incompressible MHD, equations (2.9) and (2.10), where viscous dissipation is included; i.e., $\nabla^2\omega/S_V$, where S_V is a dimensionless parameter that measures the effect of viscosity and is added to the right-hand side of equation (2.10). A general two-dimensional fixed spatial domain D is considered here (for the simulations D corresponds to the box of size $2x_{\max} \times 2y_{\max}$). Recall the ideal fluid boundary condition is

$$\boldsymbol{v} \cdot \hat{n}\Big|_{\partial D} = 0 \Rightarrow \phi\Big|_{\partial D} = \text{constant} = 0 , \tag{A1}$$

where ∂D denotes the boundary of the region D and $\hat{n}$ is the unit outward normal of D. When viscosity is included, the appropriate additional boundary condition is

$$\boldsymbol{v} \cdot \hat{t}\Big|_{\partial D} = \boldsymbol{e}_z \times \nabla\phi \cdot \hat{t}\Big|_{\partial D} = \hat{n} \cdot \nabla\phi\Big|_{\partial D} = 0 , \tag{A2}$$

where $\hat{t}$ is the unit tangent vector to the curve defining D. For the magnetic field we made use of the frozen-in boundary condition

$$\Psi\Big|_{\partial D} = \psi_E , \tag{A3}$$

which is equivalent to

$$\psi\Big|_{\partial D} = \text{constant} = 0 . \tag{A4}$$

Now we will show that the following energy-type functional satisfies the above requirements for Liapunov stability:

$$H[\phi, \psi] = \tfrac{1}{2}\int_D (|\nabla\phi|^2 + |\nabla\psi|^2)d^2x . \tag{A5}$$

The functional H is positive definite with an extremal point satisfying

$$\delta H[\phi, \psi; \delta\phi, \delta\psi] = -\int_D (\nabla^2\phi\,\delta\phi + \nabla^2\psi\,\delta\psi)d^2x + \oint_{\partial D} (\nabla\phi\,\delta\phi + \nabla\psi\,\delta\psi) \cdot \hat{n}\,ds = 0 , \tag{A6}$$

where the divergence theorem in two dimensions has been used. Note, s denotes the arc length that parametrizes the curve describing the boundary of D. Since it is assumed that ϕ and ψ are constant on ∂D, $\delta\phi$ and $\delta\psi$ vanish on the boundary and equation (A6) implies

$$\begin{aligned} \nabla^2\phi &= 0 \\ \nabla^2\psi &= 0 . \end{aligned} \tag{A7}$$

In light of the boundary conditions, the solution of equations (A7) is $\phi = 0$ and $\psi = 0$; i.e., the extremal point is the unique equilibrium point $\phi = 0$ and $\Psi = \psi_E$. Evidently, the equilibrium point is a minimum since H is positive definite. (H in fact defines a norm on the space of functions that satisfy the boundary conditions. Thus, $H > 0$ assures strong positivity, i.e., convexity.) Now consider the time derivative of H,

$$\frac{dH}{dt} = -\int_D \left(\frac{J^2}{S} + \frac{\omega^2}{S_V}\right)d^2x + \oint_{\partial D} \left[\left(\phi\nabla\frac{\partial\phi}{\partial t} + \psi\nabla\frac{\partial\psi}{\partial t} + \phi\nabla\omega - \omega\nabla\phi\right) \cdot \hat{n} + (J\phi\nabla\psi - \omega\phi\nabla\phi) \cdot \hat{t}\right]ds . \tag{A8}$$

Here use has been made of equations (2.9) and (2.10) and again the divergence theorem in two dimensions. Because of the boundary conditions the surface terms of equation (A8) vanish. The first term vanishes either because of the ideal conditions $\phi = 0$ or because of $\hat{n} \cdot \nabla\phi = 0$, while the second term vanishes because of the frozen condition $\psi = 0$. Similarly, the third, fifth, and sixth terms vanish because of the ideal boundary condition $\phi = 0$. However, the fourth term requires the nonideal condition $\hat{n} \cdot \nabla\phi = 0$. When these conditions are met, equation (A8) becomes

$$\frac{dH}{dt} = -\int_D \left(\frac{J^2}{S} + \frac{\omega^2}{S_V}\right)d^2x . \tag{A9}$$

Thus we see that $dH/dt \leq 0$ and vanishes when $J = \omega = 0$, which are precisely the conditions for the equilibrium point as given by equation (A7).

We would like to point out that the above derivation will hold for any harmonic (current-free) equilibrium state, provided that the boundary conditions (A1)–(A4) are satisfied.

In the simulations viscosity is quite small, so that it does not influence the dynamics during relaxation. Since the simulations were initialized with no perturbed velocity, the role of viscosity is minimal as the current decays resistively.

REFERENCES

Baum, P. J., & Bratenahl, A. 1974a, J. Plasma Phys., 11, 93
———. 1974b, Phys. Fluids, 17, 1232
Baum, P. J., Bratenahl, A., & White, R. S. 1973, Phys. Fluids, 16, 226
Baum, P. J., & Pollack, J. 1973, J. Appl. Phys., 44, 163
Biskamp, D. 1986, Phys. Fluids, 29, 1520
Bratenahl, A., & Yeates, C. M. 1970, Phys. Fluids, 13, 2696
Chapman, S., & Kendall, P. C. 1963, Proc. R. Soc. Lond. A, 271, 435
Craig, I. J., & McClymont, A. N. 1991, ApJ, 371, L41
———. 1993, ApJ, 405, 207
Craig, I. J., & Watson, P. G. 1992, ApJ, 393, 385
DeLuca, E. E., & Craig, I. J. 1992, ApJ, 679, 390
Drake, J. F., & Lee, Y. C. 1977, Phys. Fluids, 20, 137
Dungey, J. W. 1953, Phil. Mag., 44, 725
———. 1958, Cosmic Electrodynamics (New York: Cambridge Univ. Press), 98–102
Furth, H. P., Killeen, J., & Rosenbluth, M. N. 1963, Phys. Fluids, 6, 459
Giovanelli, R. G. 1947, MNRAS, 107, 338
Hassam, A. B. 1992, ApJ, 399, 159
Lapidus, A. 1967, J. Comp. Phys., 2, 154
Oberhettinger, F. 1972, in Handbook of Mathematical Functions, ed. M. Abramowitz & I. A. Stegun (New York: Dover)
Ofman, L. 1992, Ph.D. thesis, Univ. of Texas
Ofman, L., Chen, X. L., Morrison, P. J., & Steinolfson, R. S. 1991, Phys. Fluids, B3(6), 1364
Ofman, L., Morrison, P. J., & Steinolfson, R. S. 1993, Phys. Fluids, B5(2), 376
Parker, E. N. 1963, ApJ, 138, 552
Petschek, H. E. 1964, in AAS-NASA Symp. on Solar Flares (NASA SP-50), ed. W. N. Hess, 425
Priest, E. R. 1981, Solar Flare Magnetohydrodynamics (New York: Gordon & Breach)
Richtmyer, R. D., & Morton, K. W. 1967, Difference Methods for Initial Value Problems (2d ed; New York: Wiley-Interscience)
Rutherford, P. H. 1973, Phys. Fluids, 16, 1903
Steinolfson, R. S., Ofman, L., & Morrison, P. J. 1992, in Micro and Meso Scale Phenomena in Space Plasmas, ed. M. Ashour-Abdalla & T. S. Cheng (Washington: AGU), in press
Steinolfson, R. S., & Van Hoven, G. 1984, Phys. Fluids, 27, 1207
Steinolfson, R. S., & Winglee, K. M. 1993, J. Geophys. Res., 98, A5, 7537
Sweet, P. A. 1958, in IAU Symp. 6, Electromagnetic Phenomena in Cosmical Physics, ed. B. Lehnert (Cambridge: Cambridge Univ. Press), 123
Syrovatsky, S. I. 1966, Soviet Astron., 10, 270
———. 1971, Soviet Phys.—JETP, 33, 933
———. 1981, ARA&A, 19, 163